Anti-GBM potential of Rosmarinic acid and its synthetic derivatives via targeting IL17A mediated angiogenesis pathway

Md Shamsuddin Sultan Khan [A, C, E], Mohammad Adnan Iqbal [B], Muhammad Asif [A], Tabinda Azam [B], Majed Al-Mansoub [A], Rosenani S. M. A. Haque [B], Mohammed Khadeer Ahamed Basheer [C], Aman Shah Abdul Majid [D], Amin Malik Shah Abdul Majid [A, C, E*]

Supplementary Data

Table S1. Scoring profile of the ADME and physicochemical properties of the candidate glioblastoma drugs in NOVA program. Example of scoring criteria for CNS penetration, log(BB), for compounds intended for a CNS target.

Model	Oral CNS value	Intravenous CNS value	Lipinski rule of five	Importance
logS	> 1	--	--	0.80
HIA category	+	--	--	0.75
logP	0 to 3.5	--	--	0.60
BBB log([brain]/[blood])	-0.2 to 1	--	--	0.50
BBB category	+	--	--	0.50
P-gp category	no	--	--	0.48
hERG pIC50	≤ 5	--	--	0.40
2C9 pKi	≤ 6	--	--	0.30
2D6 affinity category	Low medium	--	--	0.30
PPB90 category	low	--	--	0.20
logS	--	> 1	--	0.80
logP	--	0 to 3.5	--	0.60
BBB log([brain]/[blood])	--	-0.2 to 1	--	0.50
BBB category	--	+	--	0.55
P-gp category	--	no	--	0.48
HIA category	--	+	--	0.40
hERG pIC50	--	≤ 5	--	0.20
2D6 affinity category	--	Low medium	--	0.18
2C9 pKi	--	≤ 6	--	0.18
PPB90 category	--	low	--	0.10
HBA	--	--	≤ 10	0.5
HBD	--	--	≤ 5	0.5
MW	--	--	≤ 500	0.5
logp	--	--	≤ 5	0.5

Table S2. IC_{50} and selectivity index (SI) of the various melanoma (cancer) cells. SI is the ratio of IC_{50} of normal cell and cancer cell. Results are presented as mean ± SEM of three separate experiments (n = 6).

Compounds	IC_{50} (μg/ml) U87 MG	IC_{50} (μg/ml) DBTRG MG	IC_{50} (μg/ml) EA.hy926	IC_{50} (μg/ml) Epithelial cell MDCK	Selectivity Index (SI)		
					U87	DBTRG	EA.hy926
NaR	154.44	--	407.13	>1000	6.47	--	2.45
AgR	1285.14	--	472.42	>1000	0.77	--	2.11
FLVM	390.37	512.22	146.45	>1000	2.56	1.95	6.82
FLVZ	208.21	417.36	91.1	>1000	4.80	2.39	10.97
RA	331.58	--	121.4	>1000	3.01	--	8.23
CA	532.83	--	144.89	>1000	1.87	--	6.90

Table S3. Effect of compounds on expression of caspases 3/7, 8, and 9. The results are mean values ± SEM (n=3).

Compounds	Caspase		
	Caspase 3	Caspase 8	Caspase 9
NaR	0.826±0.64	0.721±0.78	0.821±0.35
AgR	0.948±0.38	0.682±0.28	0.691±0.81
FLVM	0.926±0.74	0.789±0.55	0.802±0.65
FLVZ	0.987±0.52	0.843±0.33	0.796±0.22
Control	0.112±0.45	0.058±1.23	0.105±0.98

Table S4. The active site score of VEGF. The best active site was used in docking analysis.

Name	Volume ($Å^3$)	Surface ($Å^2$)	Lipo surface ($Å^2$)	Depth (Å)	Simple Score
P0	2280.96	2431.33	1459.52	27.59	0.64
P1	793.72	914.47	518.68	19.78	0.51
P2	584.53	959.73	583.64	18.47	0.39
P3	533.36	718.22	397.56	17.28	0.34
P4	376.26	606.32	368.16	13.28	0.24
P5	261.43	569.12	399.98	13.88	0.17
P6	229.53	282.34	193.32	10.12	0.08
P7	217.17	458.76	332.63	9.48	0.14
P8	211.72	330.50	222.04	9.53	0.03
P9	209.73	359.40	225.95	10.99	0.08
P10	205.21	316.96	210.07	8.84	0.03
P11	178.49	348.43	204.79	7.79	0.00

P12	171.45	359.66	224.14	8.62	0.03
P13	171.05	334.66	201.41	8.85	0.03
P14	168.00	271.48	134.44	6.83	0.00
P15	166.80	362.24	227.70	8.45	0.02
P16	146.73	433.12	245.54	10.24	0.00
P17	138.09	226.47	135.36	8.32	0.00
P18	107.66	300.11	163.08	7.59	0.00

Table S5. The active site score of IL17A. The best active site was used in docking analysis.

Name	Volume (Å^3)	Surface (Å^2)	Lipo surface (Å^2)	Depth (Å)	Simple Score
P0	1038.40	1096.81	713.19	20.98	0.67
P1	495.42	679.37	429.24	16.90	0.29
P2	147.78	370.27	183.43	8.40	0.00
P3	143.17	332.99	190.64	7.68	0.00
P4	143.04	299.75	158.57	10.27	0.00
P5	114.18	257.46	179.83	6.50	0.00
P6	107.46	221.80	133.51	6.76	0.00

Table S6. QSAR dataset that was used to develop the QSAR model. Training set was collected from PubChem and ChemBL database.

No.	Compounds	pIC50	MW	Mol.Weight	Clean energy	logP	PSA
1	5798	2.432	1.922	118.053	4.042	1.190	28.700
2	312693	2.568	2.379	146.084	4.477	1.717	17.800
3	595193	2.568	2.623	161.095	4.897	1.303	43.800
4	606669	2.703	3.161	194.084	4.557	3.131	17.800
5	667551	2.568	3.519	216.137	6.348	1.467	33.100
6	745066	2.703	3.324	204.137	4.817	0.975	47.100
7	785141	2.703	3.858	235.995	5.255	2.968	17.800
8	797055	2.703	3.960	243.174	4.835	3.054	29.800
9	799602	2.488	2.851	175.111	4.838	1.760	43.800
10	805647	2.703	3.080	189.127	4.208	1.380	21.100
11	923821	2.703	3.633	223.111	4.522	2.821	29.800
12	1485489	2.568	2.623	161.095	4.045	1.665	40.700
13	2773179	2.703	3.748	230.153	6.323	1.803	24.300
14	3920849	2.703	2.851	175.111	4.203	0.940	43.800
15	6603577	2.568	3.412	209.072	4.614	1.561	43.800
16	13623334	2.703	4.204	258.184	7.416	2.717	24.300
17	13623357	2.703	4.677	287.211	8.004	1.967	36.300
18	18552837	2.388	3.624	222.092	5.522	0.000	8.800
19	44307771	2.703	3.943	242.153	7.382	2.174	33.100
20	44429844	2.703	7.673	470.230	5.457	0.000	8.800
21	52945375	2.568	3.960	243.174	5.113	2.674	8.800
22	71463195	2.703	3.960	243.174	5.113	2.674	21.100
23	90664974	2.703	4.445	272.060	7.216	1.630	42.200
24	Ethyl	2.658	2.379	146.080	5.141	1.699	35.000
25	Propyl	2.658	2.607	160.100	5.081	2.157	42.000
26	Butyl	2.658	2.835	174.120	5.053	2.622	40.000
27	Pentyl	2.613	3.063	188.130	5.043	3.080	35.000
28	Hexyl	2.613	3.292	202.150	5.012	3.537	20.000
29	Heptyl	2.658	3.520	216.160	4.983	3.994	35.000

30	CHEMBL1095048	6.300	3.000	278.300	5.300	1.700	59.800
31	CHEMBL1087494	6.400	2.000	308.330	4.005	1.700	69.000
32	CHEMBL1087495	6.400	1.000	356.500	5.002	5.200	59.800
33	CHEMBL96951	4.700	2.000	297.280	7.024	2.800	66.400
34	CHEMBL192441	6.800	2.000	344.410	6.000	2.700	42.600
35	CHEMBL194651	7.300	1.000	378.480	5.022	3.800	42.000
36	CID 700009	5.700	3.000	209.240	3.000	3.400	36.000
37	CHEMBL139430	10.500	2.000	316.350	3.000	3.100	94.000
38	CHEMBL139485	10.300	3.000	356.370	5.000	1.800	122.000
39	CHEMBL139188	8.000	3.000	252.270	4.000	1.700	103.000
40	CHEMBL141698	10.500	2.000	326.350	3.000	1.800	112.000
41	CHEMBL337603	10.500	2.000	326.350	2.000	1.800	112.000

Table S1 Detection of RA derivatives in mice brain and blood

RA derivatives	**Concentration in Brain (μg/g tissue)**	**Concentration in Blood (μg/g tissue)**
NaR	1.50±0.18	2.50±0.37 – 1.01±0.07
AgR	3.75±0.56	
FLVM	2.68±0.71	
FLVZ	3.05±0.33	

Table S2 Maximum concentration (C_{max}) and half-life ($T_{1/2}$) of RA derivatives (AgR and FLVM)

Pharmacokinetics	**AgR**	**FLVM**
C_{max}	30.01 μg/ml	14.65 μg/ml
$T_{1/2}$	1.53 h	1.7 h
Kel	0.45	0.387
Ka	58.12	30.38
MRT(AUC/AUMC)	2.21	2.57(78.37/202.17)
Cl	0.388	0.637
V	0.86	1.64

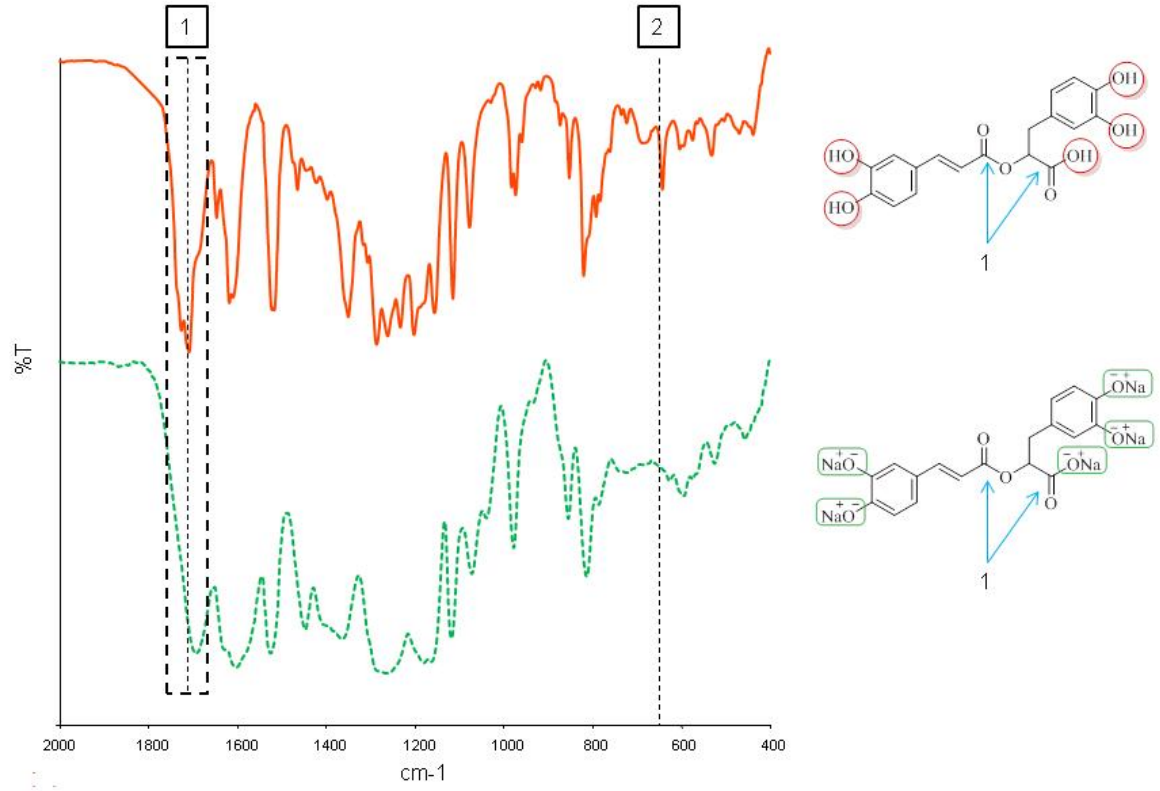

Fig. S1. FT-IR spectra of rosmarinic acid and sodium rosmarinate (NaR) in comparison. The highlighted region "1" shows noticeable changes indicating the formation of a relatively broader and single vibrational band for carbonyl groups compared to the two carbonyl vibrational bands in rosmarinic acid. In addition, in sodium rosmarinate, the carbonyl band shifted to a lower frequency compared to this band in rosmarinic acid. Furthermore, several other changes can be observed in both the spectra. For example, the vibrational band labelled as "2" disappeared in sodium rosmarinate.

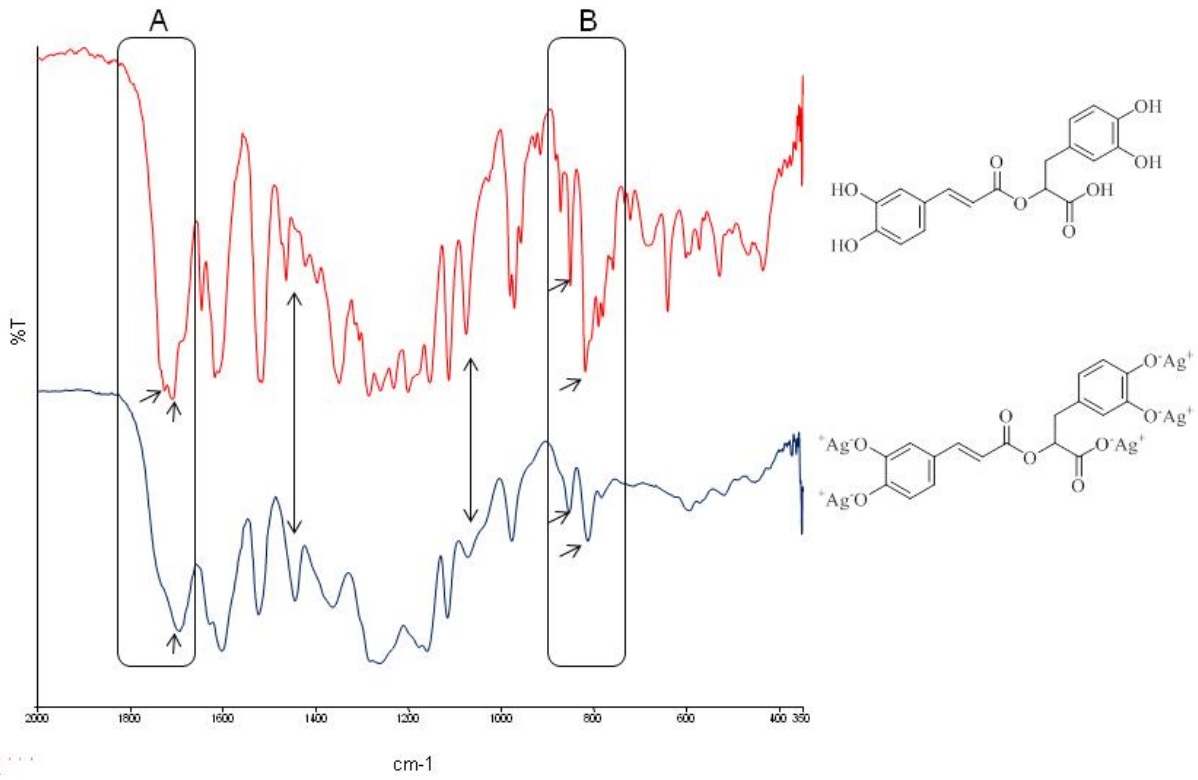

Fig. S2. FT-IR spectra of rosmarinic acid (RA) and silver rosmarinate (AgR) collected using KBr disc method. Only selected region (350 – 2000 cm^{-1}) has been shown for comparison purpose. Significant changes can be observed in the FT-IR spectrum of AgR. For example, highlighted regions A and B show observable changes in comparison. Region A is specific for the carbonyl stretch, two vibrational bands in RA for two

different types of carbonyl groups changed to a single vibrational band in AgR. Such changes have been previously reported after the replacement of either carboxylic or phenolic protons by silver or potassium ions (Jafari et al., 2014; Syed et al., 2015).

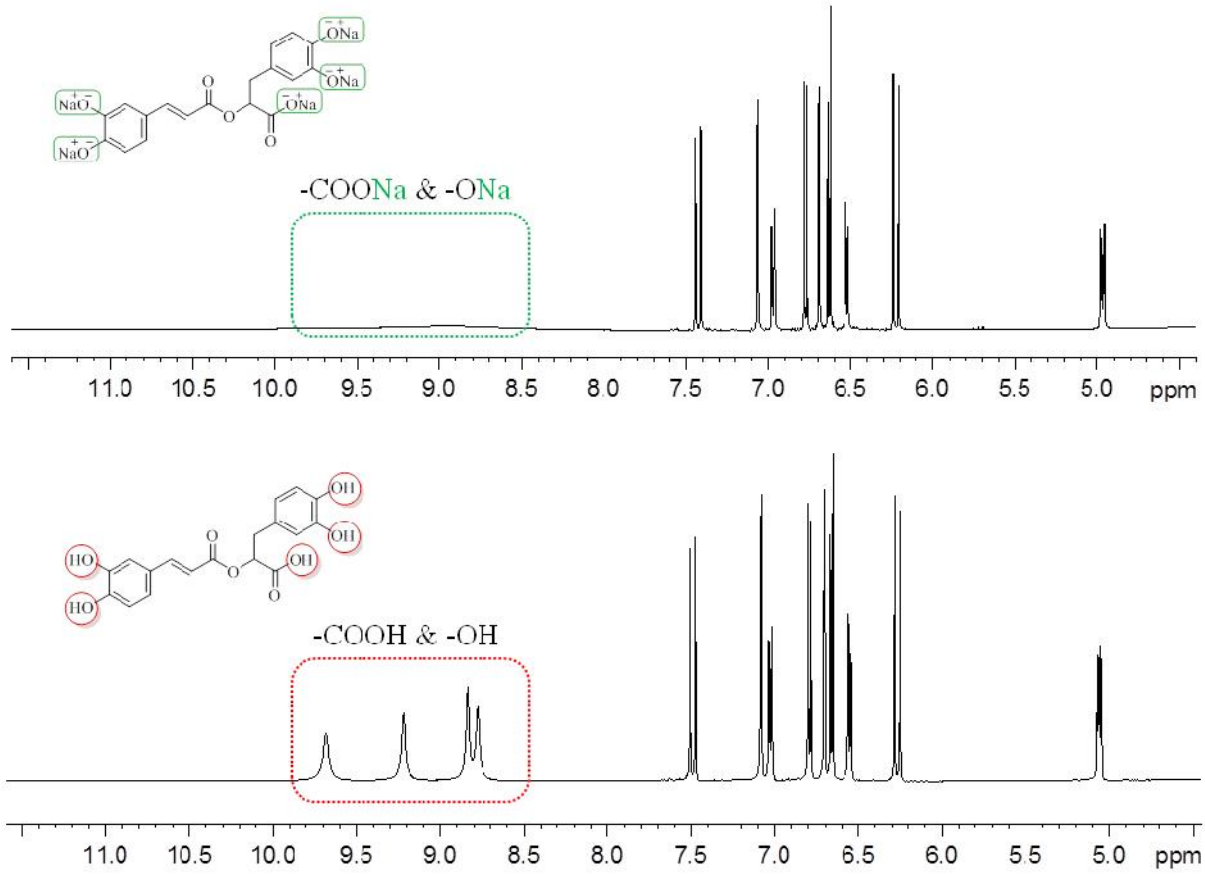

Fig. S3. Selected regions of ^{1}H NMR spectra of rosmarinic acid (RA, lower spectrum) and sodium rosmarinate (NaR, upper spectrum) collected by 500 MHz MHz NMR machine in deuterated-DMSO. The spectra in comparison clearly show that after replacement of phenolic and carboxylic protons by sodium ions, the respective chemical shifts disappeared indicating the formation of desired compound.

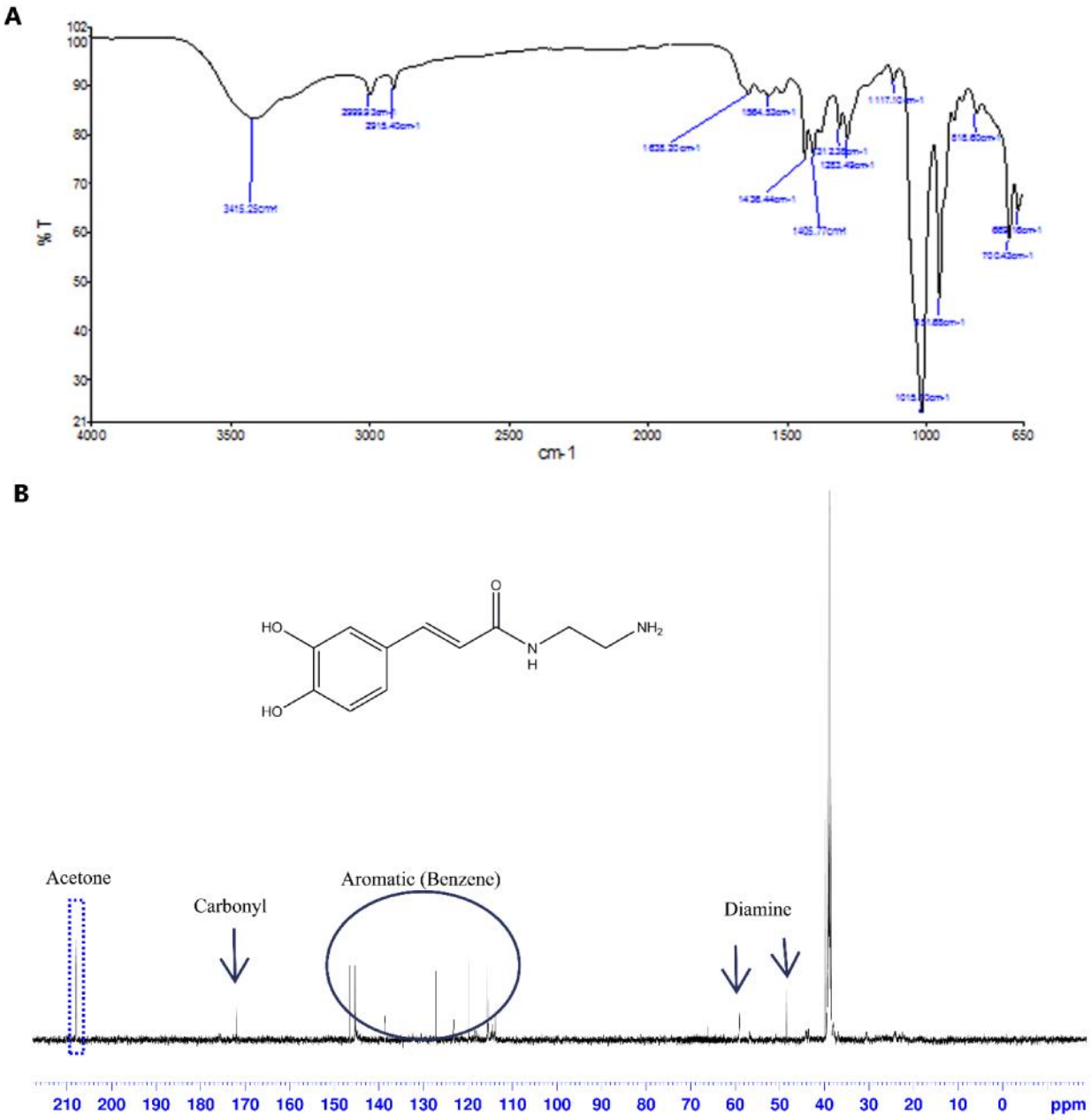

Fig. S4. Characterization of FLVM using FTIR (A) and NMR (B) imaging.

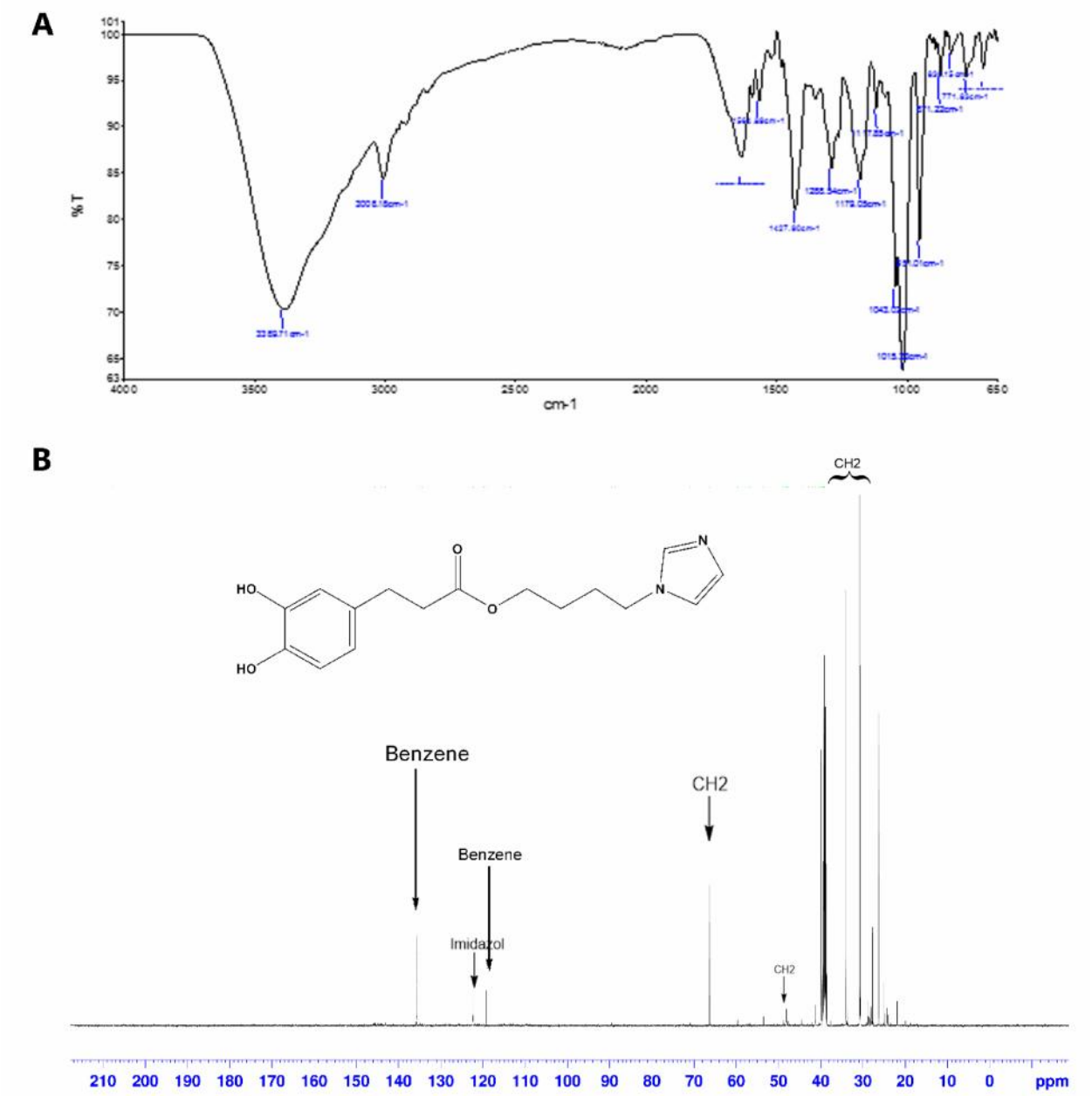

Fig. S5. Characterization of FLVZ using FTIR (A) and NMR (B) imaging.

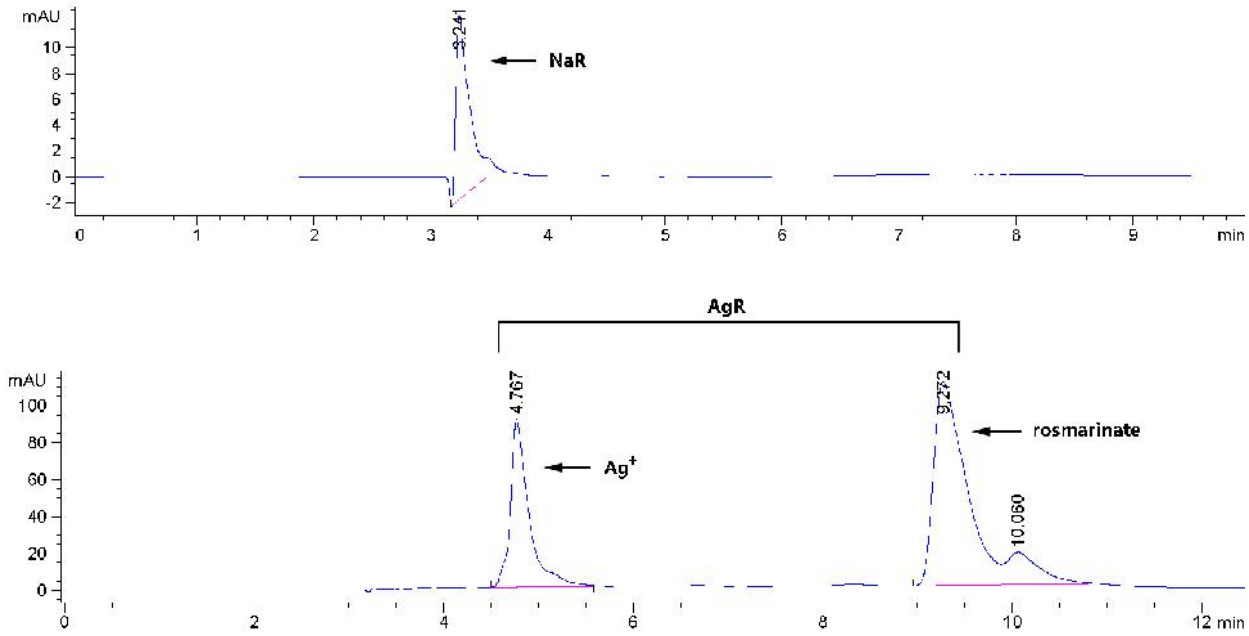

Fig. S6. Stability of the compounds determined by quality of HPLC peak. HPLC chromatogram of NaR and AgR salt in non-aqueous media. The salts were detected from in normal storage conditions. They were also detected after chemical and temperature treatments. The HPLC method cannot detect the salt and ion from aqueous media. The dissociated Ag and Na ion and the rosmarinic acid were detected by mass spectrometry.

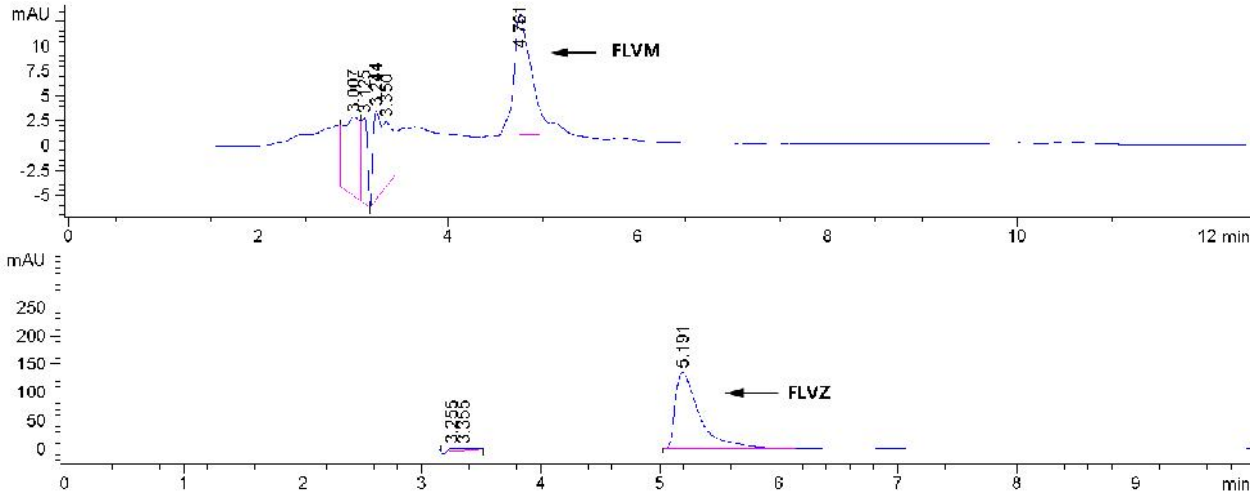

Fig. S7. Stability of the compounds determined by quality of HPLC peak. HPLC chromatogram of FLVM (A) and FLVZ (B).

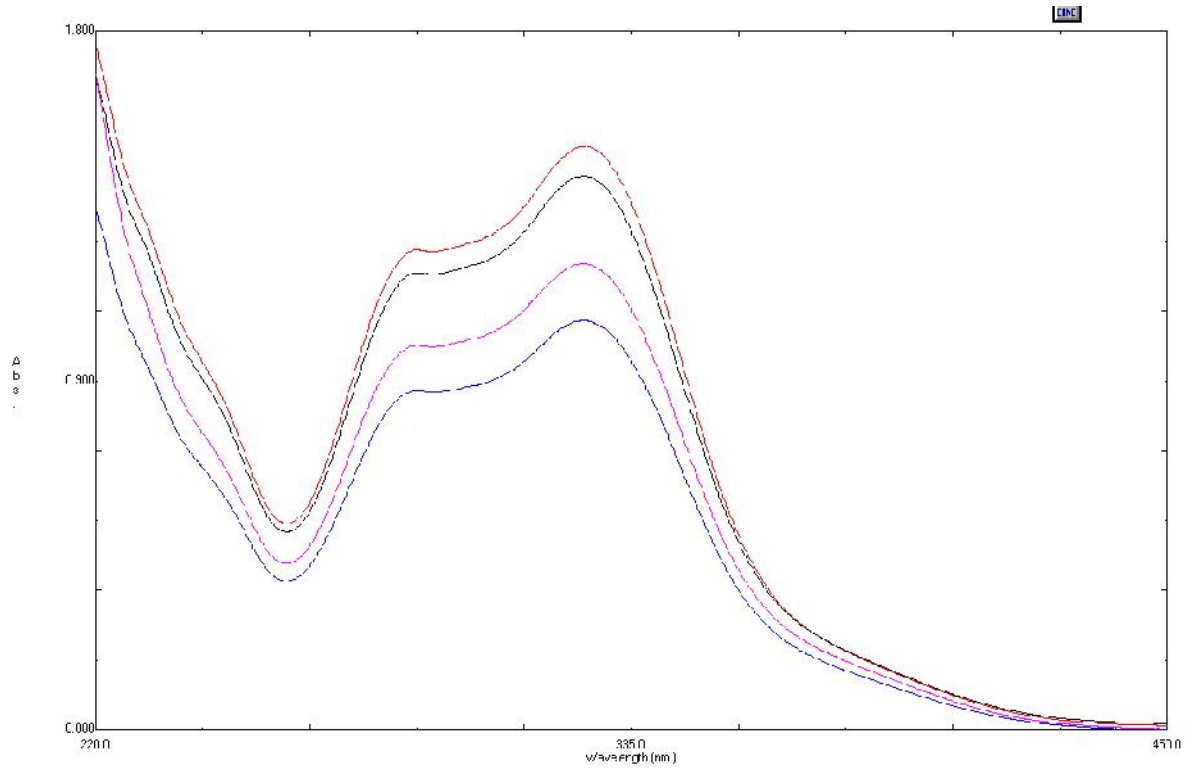

Fig. S8. Determination of logP of the compounds. UV-vis spectra of rosmarinic acid in PBS solution. red: before partition with n-octanol, black: after partition (4 ml PBS solution + 6 ml n-octanol), purple: after partition (2 ml PBS solution + 20 ml n-octanol), blue: after partition (3 ml PBS solution + 50 ml n-octanol)

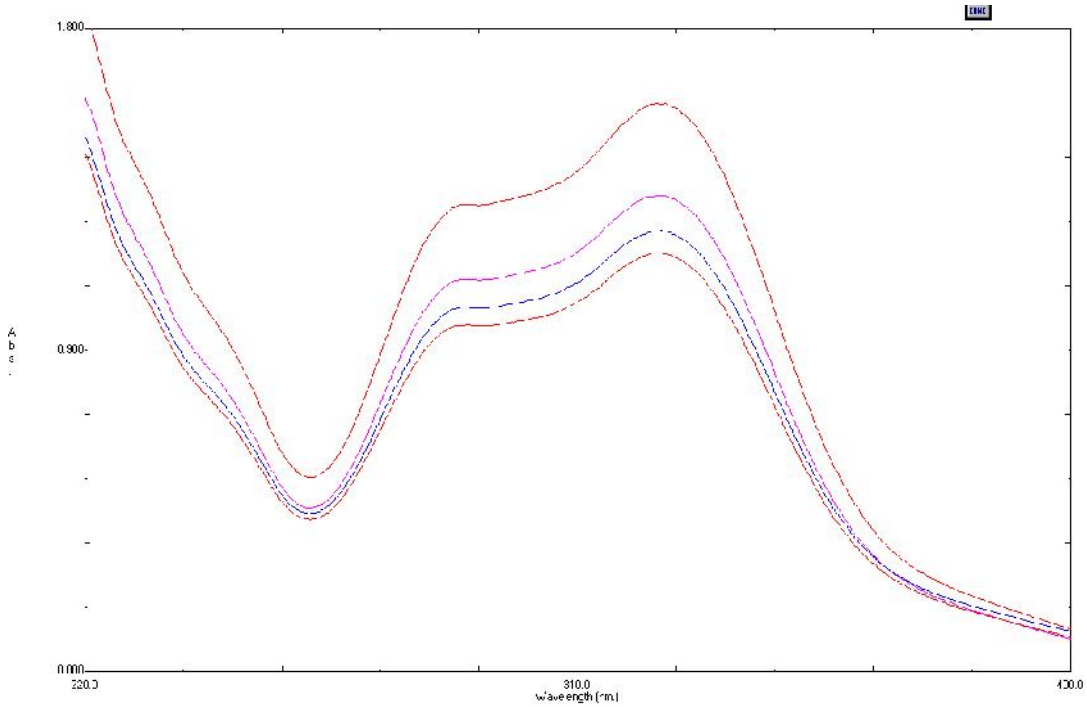

Fig. S9. Determination of logP of the compounds. UV-vis spectra of NaR in PBS solution. red: before partition with n-octanol, purple: after partition (1 ml PBS solution + 10 ml n-octanol), blue: after partition (1 ml PBS solution + 12 ml n-octanol), red: after partition (1 ml PBS solution + 18 ml n-octanol).

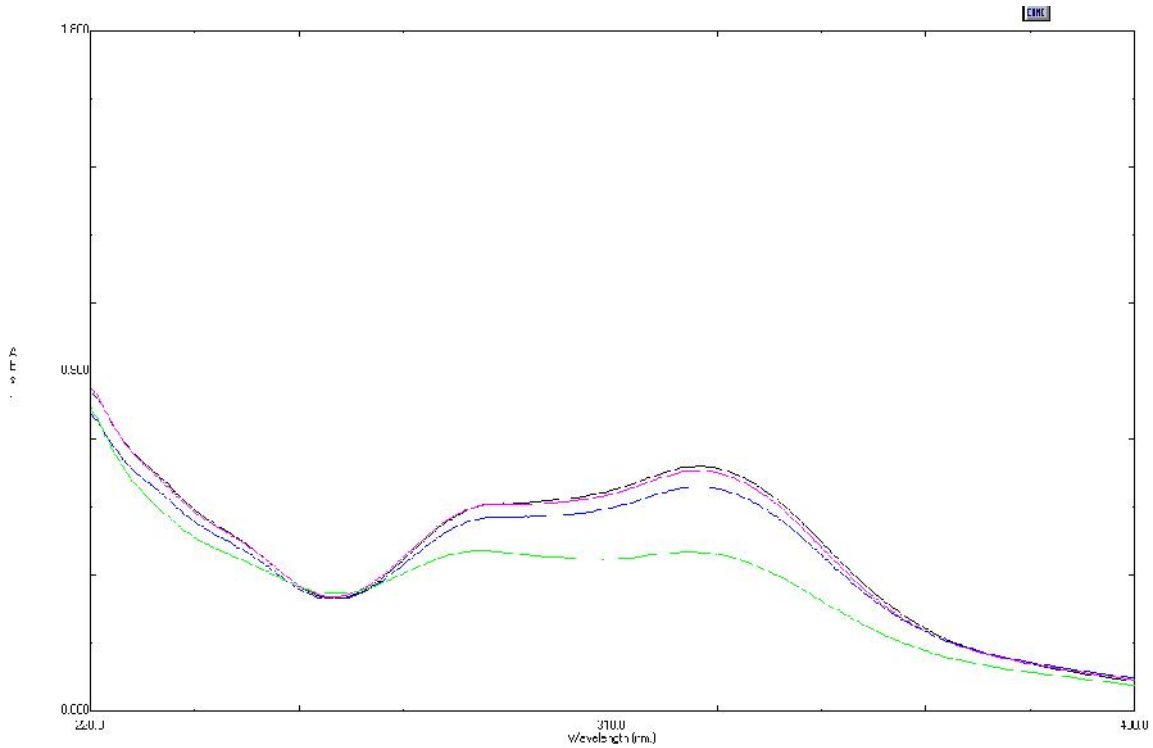

Fig. S10. Determination of logP of the compounds. UV-vis spectra of AgR in PBS solution. black: before partition with n-octanol, red: after partition (1 ml PBS solution + 5 ml n-octanol), blue: after partition (1 ml PBS solution + 12 ml n-octanol), green: after partition (1 ml PBS solution + 20 ml n-octanol).

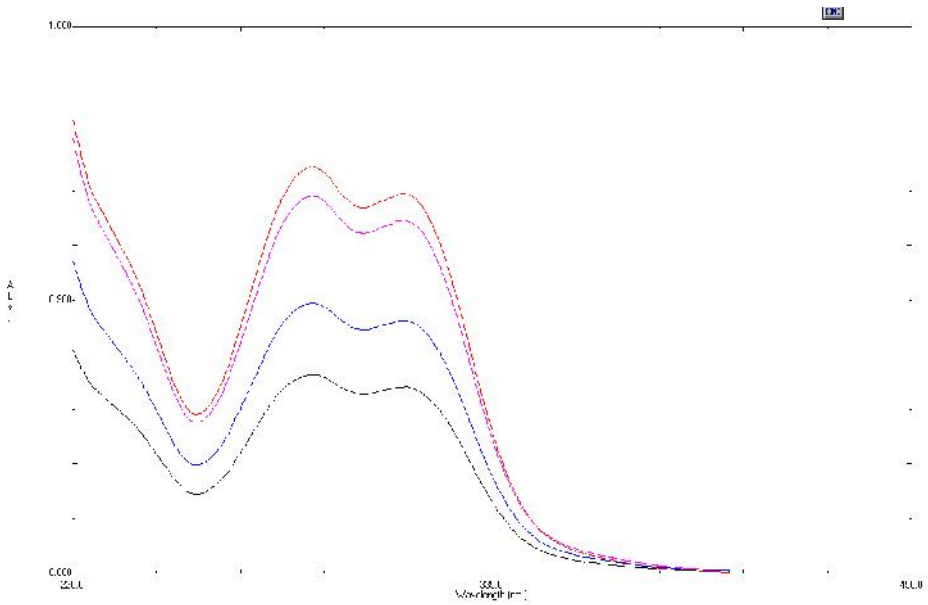

Fig. S11. Determination of logP of the compounds. UV-vis spectra of caffeic acid in PBS solution. red: before partition with n-octanol. purple: after partition (2 ml PBS solution + 2 ml n-octanol). blue: after partition (2 ml PBS solution + 10 ml n-octanol). black: after partition (1 ml PBS solution + 10 ml n-octanol).

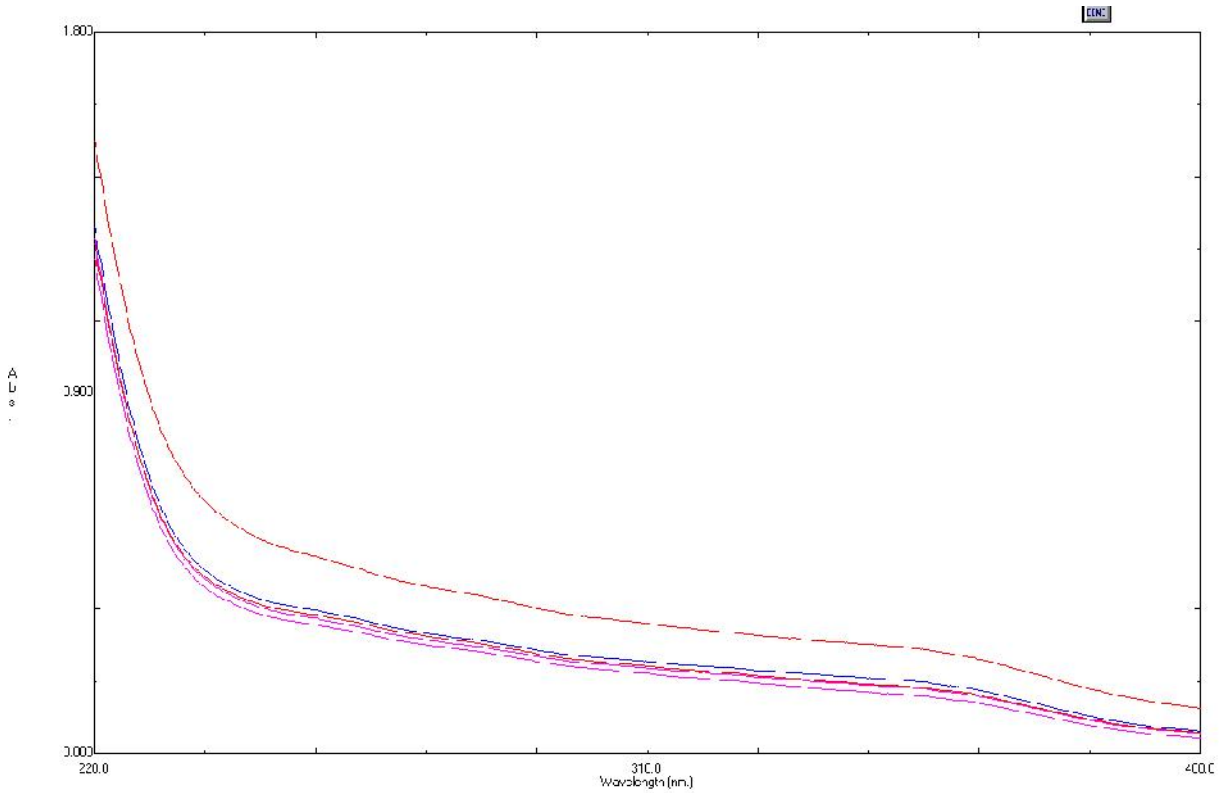

Fig. S12. Determination of logP of the compounds. UV-vis spectra of FLVZ in PBS solution. red: before partition with n-octanol. blue: after partition (5 ml PBS solution + 2 ml n-octanol). red: after partition (4 ml PBS solution + 4 ml n-octanol). purple: after partition (4 ml PBS solution + 7 ml n-octanol).

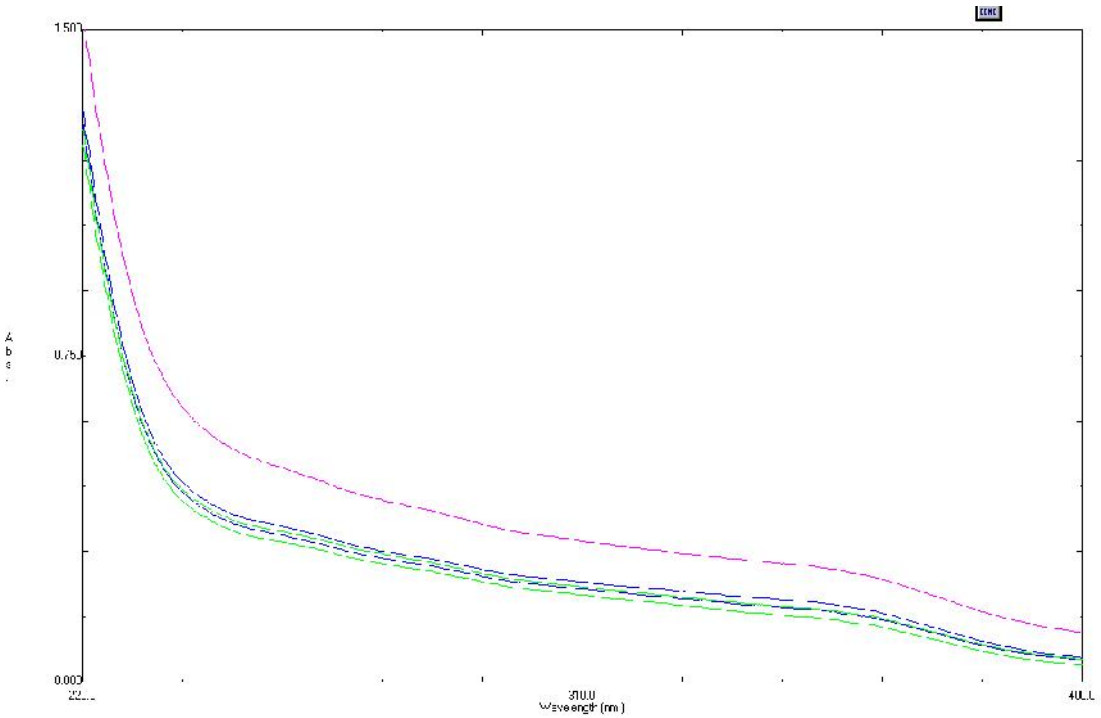

Fig. S13. Determination of logP of the compounds. UV-vis spectra of FLVM in PBS solution. purple: before partition with n-octanol. blue: after partition (2 ml PBS solution + 10 ml n-octanol). green: after partition (1 ml PBS solution + 10 ml n-octanol). green: after partition (1 ml PBS solution + 20 ml n-octanol).